SLAC–PUB–8471
SCIPP 00/19
June 2000

# The Assembly of the Silicon Tracker of the Beam Test Engineering Model of the GLAST Large Area Telescope *

P. Allport,[1] E. Atwood,[2] W. Atwood,[2] G. Beck,[3] B. Bhatnager,[4] E. Bloom,[4] J. Broeder,[4] V. Chen,[2] J. Clark,[2] N. Cotton,[2] E. do Couto e Silva,[4]† B. Feerick,[4] B. Giebels,[4] G. Godfrey,[4] T. Handa,[4] J.A. Hernando,[2] M. Hirayama,[2] R.P. Johnson,[2] T. Kamae,[5] S. Kashiguine,[2] W. Kroeger,[2] C. Milbury,[2] W. Miller,[7] O. Millican,[4] M. Nikolaou,[4] M. Nordby,[4] T .Ohsugi,[6] G. Paliaga,[2] E. Ponslet,[7] W. Rowe,[2] H.F.-W Sadrozinski,[2] E. Spencer,[2] S. Stromberg,[2] E. Swensen,[7] M. Takayuki,[4] D. Tournear,[4] A. Webster,[2] G. Winkler,[2] K. Yamamoto,[8] K. Yamamura,[8] S. Yoshida,[6]

[1] *University of Liverpool, Liverpool, L69 eBX, England, UK*
[2] *SCIPP, University of California at Santa Cruz, Santa Cruz, CA, 95064, USA*
[3] *Queen Mary and Westfield College, University of London, London, E1 4NS, England, UK*
[4] *Stanford Linear Accelerator Center, Stanford, CA, 94309, USA*
[5] *University of Tokyo, Tokyo 113–0033, Japan*
[6] *Hiroshima University, Higashi–Hiroshima 739–8526, Japan*
[7] *Hytec Inc., Los Alamos, NM, 87544, USA*
[8] *Hamamatsu Photonics, Hamamatsu 430-8587, Japan*

**Abstract**

The silicon tracker for the engineering model of the GLAST Large Area Telescope(LAT) to date represents the largest surface of silicon microstrip detectors assembled in a tracker (2.7 $m^2$). It demonstrates the feasibility of employing this technology for satellite based experiments, in which large effective areas and high reliability are required. This note gives an overview of the assembly of this silicon tracker and discusses in detail studies performed to track quality assurance: leakage current, mechanical alignment and production yields.

*Presented at the 4$^{th}$ International Symposium on Development and Application of Semiconductor Tracking Detectors, March 20-25 2000, Hiroshima, Japan*

*Work supported by Department of Energy contract DE–AC03–76SF00515 and NASA grant NCC5–195.
†Corresponding author. Tel. +1 650 926 2698, email: eduardo@slac.stanford.edu

# 1 Introduction

The Gamma Ray Large Area Space Telescope (GLAST) mission is a next generation satellite based gamma ray experiment [1] and is scheduled to be launched in 2005. GLAST is designed to address fundamental issues of particle physics, astrophysics and cosmology, by probing a region of gamma ray energies between 30 MeV and 300 GeV, which has not yet been explored in detail by current experiments. A description of the scientific objectives of GLAST has been given in these proceedings [2].

The silicon tracker for the GLAST Large Area Telescope (LAT) will consist of more than one million readout channels, distributed over 74 $m^2$ of silicon. To verify the performance of the design and validate the reliability and integration of the instrument, we built a beam test engineering model (BTEM). This corresponds structurally to 1/16 of the GLAST LAT and consists of about 4% of the silicon surface of the final instrument. This detector was installed in a test beam of positrons, hadrons and tagged photons at SLAC in December of 1999 and January of 2000. The construction of this tracker has already been described in [3]. In this paper we will focus on particular issues of construction concerning the silicon detectors, such as leakage current measurements, mechanical alignment and production yields.

# 2 Silicon tracker

The Silicon tracker for the BTEM consists of 41600 readout channels wire bonded to 2.7 $m^2$ of single sided silicon detectors assembled into ladders. Typical ladders used for high energy experiments have a carbon fiber structural support. However in the GLAST design, the stiffness of ladders during assembly is guaranteed by edge bonding detectors along their thin sides as shown in Fig 1.

After ladders have been edged glued, strips are wirebonded and leads are encapsulated. A thermal treatment follows encapsulation for curing of the adhesive. Only then are ladders placed manually into 17 mechanical modules labeled trays, which provided structural support (see Fig 2). Each tray consists of 2 layers of detectors whose strips are oriented along the same direction. Thin lead converters preceed the bottom layer of detectors.

Fig 3 depicts the layout of the silicon tracker. Trays with strips along $x$ and $y$ directions alternate throughout the tracker, thus creating pairs of $x$ and $y$ coordinate measurements right after each converter. The topmost and bottommost layers of the tracker are not instrumented with silicon detectors. The three bottom layers are not equipped with lead converters because the tracking trigger requires $3x$ and $3y$ layers in coincidence after the conversion point. In addition, the material of the converter would degrade the angular and energy resolution for detecting photons. Therefore, a total of 32 layers (16 planes) of single sided silicon microstrip detectors are read out by the electronic boards mounted on the sides of the trays. Details on the front-end electronics have been discussed in these proceedings [4].

# 3 Silicon Detectors

The silicon tracker employs single sided silicon detectors with 194 $\mu$m strip pitch patterned on high resistivity 400 $\mu$m-thick $n$–type substrates. There were 550 detectors ordered from Hamamatsu Photonics. They correspond to 296 detectors from 4 inch wafers and 254 from 6-inch wafers, whose dimensions are 64.0 mm $\times$ 64.0 mm and 64.0 mm $\times$ 106.8 mm, respectively. In addition we also received 5 detectors of 64.0 mm $\times$ 106.8 mm with the similar design manufactured by Micron Semiconductor Ltd. The leakage current and the number of defective strips for all detectors has been measured by the manufacturer before delivery.

# 4 Leakage Current

For all results in this note the leakage current measurements were performed at 100 V. Our quality assurance procedures required testing of either detector current or coupling capacitors after step of integration in which either of them could have changed. Changes could come from mechanical stresses, mishandling or contamination. During ladder production the leakage current was measured for

- Detectors: upon delivery (before edge gluing),
- Detectors: after edge gluing (before wire bonding)
- Ladders: after wire bonding,
- Ladders: after encapsulation of wirebonds.

## 4.1 Detectors

Figure 4 shows the leakage current for each detector measured by the GLAST collaboration. One can clearly see the dependence on different detector batches. The first batch from 4–inch wafers (top) shows in average higher leakage current than that obtained in the second batch (middle). The batch from 6–inch wafers (bottom), indicates that despite of the large area of silicon detectors, the leakage current values are still very low. This clearly indicates that the leakage current is not a function of the area and thickness alone but depends also on the details of the processing steps.

## 4.2 Ladders

Figure 5 shows the ratio of ladder leakage currents after and before edge gluing for all but 2 ladders. Since this distribution is characterized by a mean of 1.08 and $rms$ of 0.28, we conclude that edge gluing does not affect the electrical properties of the detectors. Nevertheless there were 2 ladders, not shown in Fig. 5, whose leakage current increased beyond a factor of 2. Since the current for these ladders remained stable they were used later for production.

Figure 6 shows the ratio of ladder currents after and before wire bonding. The mean ratio is 1.61 with the $rms$ value of 0.41. We conclude that wire bonding increases leakage

| Ladder | Final leakage current ($\mu$A) | Comments |
|---|---|---|
| 38 | 111.9 | rejected |
| 50 | 34.9 | accepted |
| 134 | 24.1 | rejected |
| 139 | 8.8 | accepted (stable current) |

Table 1: Ladders with leakage current greater than 5 $\mu$A after final assembly.

current by a factor of 1.6 . There were also 15 ladders, not shown in Fig 6, whose leakage current increased by more than a factor of 3. The leakage current for these ladders were shown to be stable except for one (ladder 134), which was rejected due to further increase in leakage current after encapsulation of wire bonds.

Figure 7 shows the ratio of ladder currents after and before encapsulation of wire bonds. The distribution is characterized by a ratio of 0.92 with and $rms$ of 0.29 and indicates no changes in leakage current due to encapsulation of wire bonds. Note that the distribution tends to slightly pull towards values less than 1. This may imply that either time has a beneficial effect in reducing leakage current or heating detectors reduces leakage current from surface moisture. We do not have enough information to disentangle both effects. Encapsulation also triggered increase in leakage current by a factor greater than 2 (not shown in Fig 7) for 5 ladders and worsened considerably the current of ladder 134.

Table 1 shows the leakage current for ladders whose leakage current was greater than 5 $\mu$A after final assembly. Ladders 38 and 134 have been rejected. Ladder 50 was used for final assembly so that we could study its effect on the electronics. Ladder 139, made with Micron detectors, had stable leakage current and was accepted for final production.

Figure 8 displays the leakage current for all ladders with leakage current less than 5 $\mu$A after ladder assembly (ladders with higher currents have been described in Table 1). Those using detectors from 6 inch wafers (bottom) have lower leakage current than those from 4 inch wafers (top). This is the largest sample to date of high quality detectors from 6 inch wafers and proves the high reliability of this technology. The superior behavior of the ladders made from 6–inch wafers can be ascribed to two factors: lower leakage current and smaller number of detectors used per ladder (3 instead of 5). During the two months of operation in the test beam with a bias volateg of 100 V, the total leakage current remained stable and consistent with the expect values from the sum of the leakage current of the individual ladders.

## 4.3 Mechanical Alignment

Since the ladder assembly required placement of detectors against pins (see Fig. 9), the alignment of detector in ladders relied on precise dicing of silicon wafers. Detectors were edge bonded with epoxy and heated for 2 hours at 60°C. The maximum deviations seen for all ladders are shown in Fig. 9. We measured the location of the four detector corners and

calculated the average misalignment of detectors in a ladder to be the order of 22 $\mu$m.

Only one ladder was rejected due to large misalignments ($>$ 100 $\mu$m), but there were few ladders with misalignments greater than 50 $\mu$m, which suggests we need to improve our process control. After ladders were glued onto trays, the detector fiducial marks were also used for the survey. Fig 10 shows the difference between nominal and measured positions which are perpendicular to the orientation of the strips. This does not provide information about rotations of ladders. Rotations were measured with respect to the edge of the trays to be the order of 50 $\mu$m indicating that our assembly procedure needs to be modified [3]. After trays were built they were stacked to form a tower, which was then surveyed along the $z$ coordinate. The aluminum closeouts were measured to be within $\pm$ 100$\mu$m of their nominal positions and planarity of about 12 $\mu$m over the length of the tray was achieved.

# 5 Yield

A detailed description of production yields and repairs can be found in [3]. The number of defective strips seen after final assembly was 25, which corresponds to 0.06% of the total number of 32 cm long strips. For the detector yield we assumed that if a given ladder was rejected to due increase in leakage current, all detectors in that ladder were considered not of good quality [3]. The combined detector yield was 96.5%, where for the detectors from 4 inch wafers we obtained 94.6% and for those from 6 inch wafers, 98.8%. Finally ladder yield went from 93.2% to 97.7% due to ladder repairs. Similar yields have been obtained before for a different detector [5]. These results combined indicate the high reliability and maturity of silicon technology and the benefits of careful planning of the assembly procedures.

# 6 Conclusion

The assembly steps of the silicon tracker for the beam test engineering model of GLAST has been monitored with leakage current measurements.

During ladder assembly the only significant increase in leakage current was a factor of 1.6 after wirebonding. Although after wirebonding the leakage current of 15 detectors increased by more than a factor of 3, 14 of those had stable and/or reduced leakage current after final assembly. After encapsulation of wire bonds the leakage current of the only ladder affected by wirebonding increased even further and the ladder was rejected. In addition, two other ladders had runaway leakage currents and were also rejected.

Detectors were aligned in ladders with a precision of about 22 $\mu$m. However, the precision of assembly of ladders into trays were the order of 50 $\mu$m and clealy has to be improved. The construction of the BTEM silicon tracker demonstrates the feasibility of employing 6 inch technology for satellite based experiments, in which high reliability and large effective areas are required.

**Acknowledgments**

We thank the organizers of the Hiroshima Conference for such a pleasant stay and the high level of discussions. We thank the SLAC directorate for their strong support to this experiment. Work supported by U.S. Department of Energy, contract DE-AC03-76SF00515 and NASA grant NCC5–195.

# References

[1] P. Michelson *et al.*, Proc. SPIE, Vol **2806** (1996) 31.

[2] H. F-W. Sadrozinski *et al.*, *GLAST, The Gamma Ray Large Area Space Telescope*, these proceedings.

[3] E. Atwood *et al.*, *The Silicon Tracker of the Beam Test Engineering Model of the GLAST Large Area Telescope*, SLAC–PUB–8466, June 2000. Submitted to Nucl. Inst. and Meth. **A**

[4] V. Chen *et al.*, *The Readout Electronics for the GLAST Silicon-Strip Pair-Conversion Tracker*, these proceedings.

[5] G. Barichello *et al.*, Nucl. Inst. and Meth. **A 413** (1998) 17.

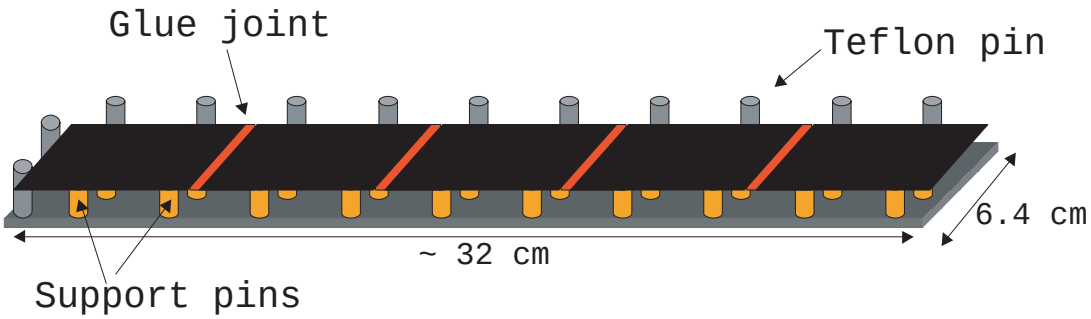


Figure 1: Schematic drawing of ladder assembly fixture

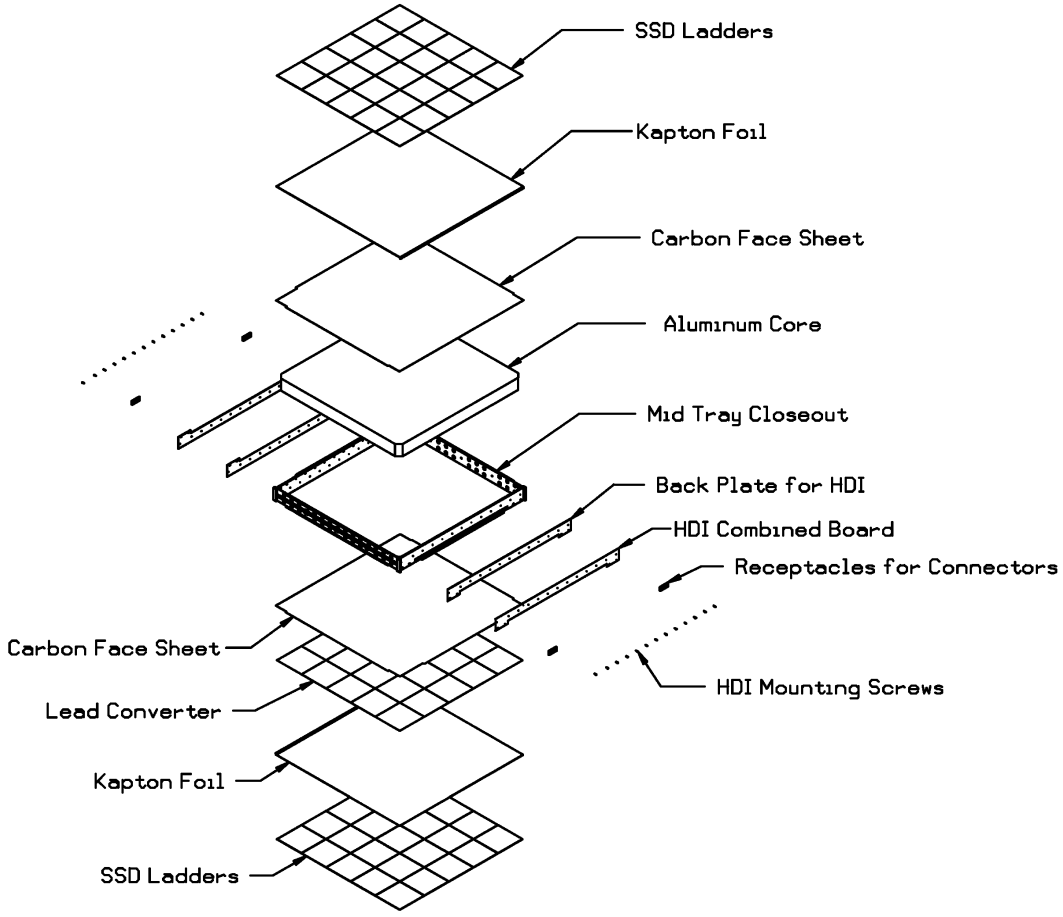


Figure 2: Exploded view of the mechanical layout of a tray.

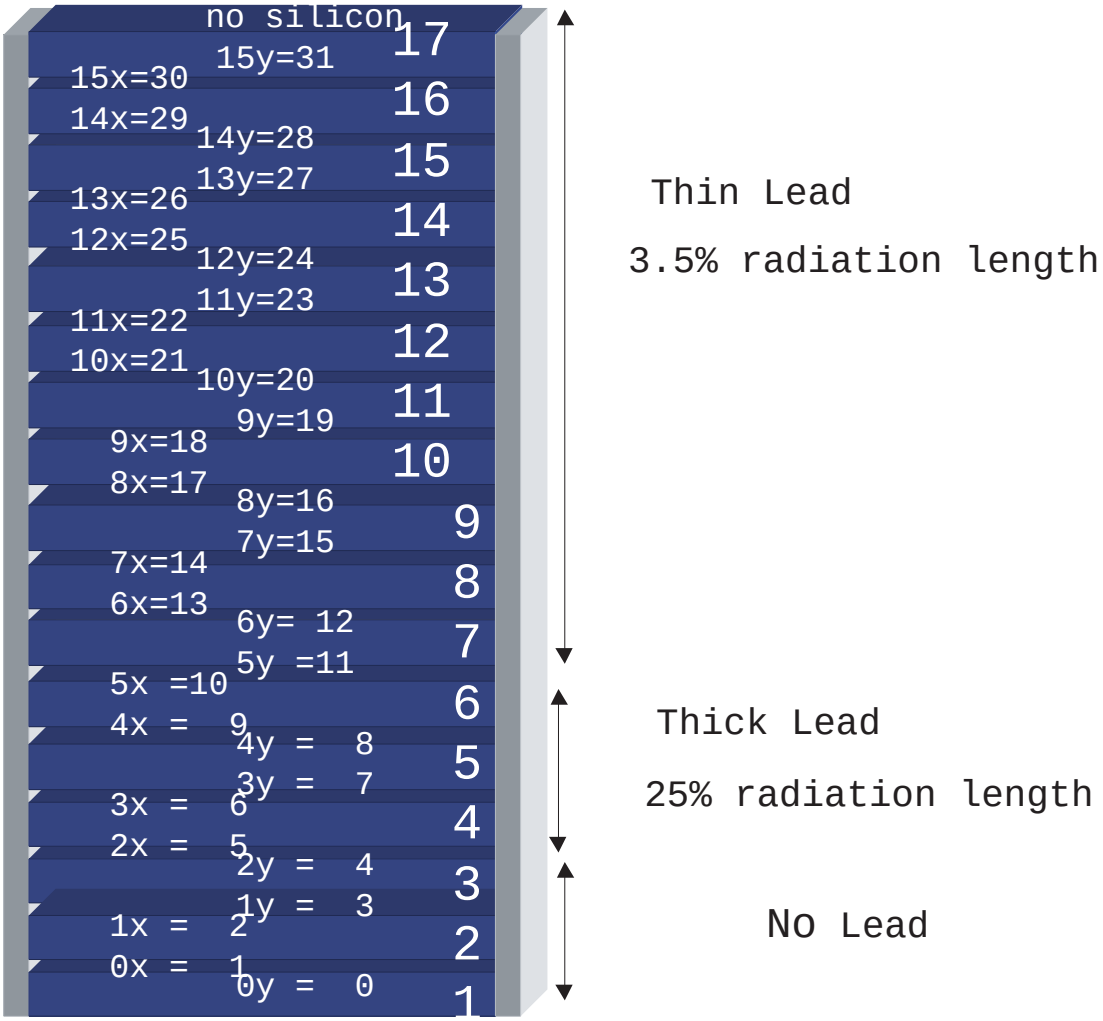


Figure 3: Schematic drawing of the GLAST silicon tracker.

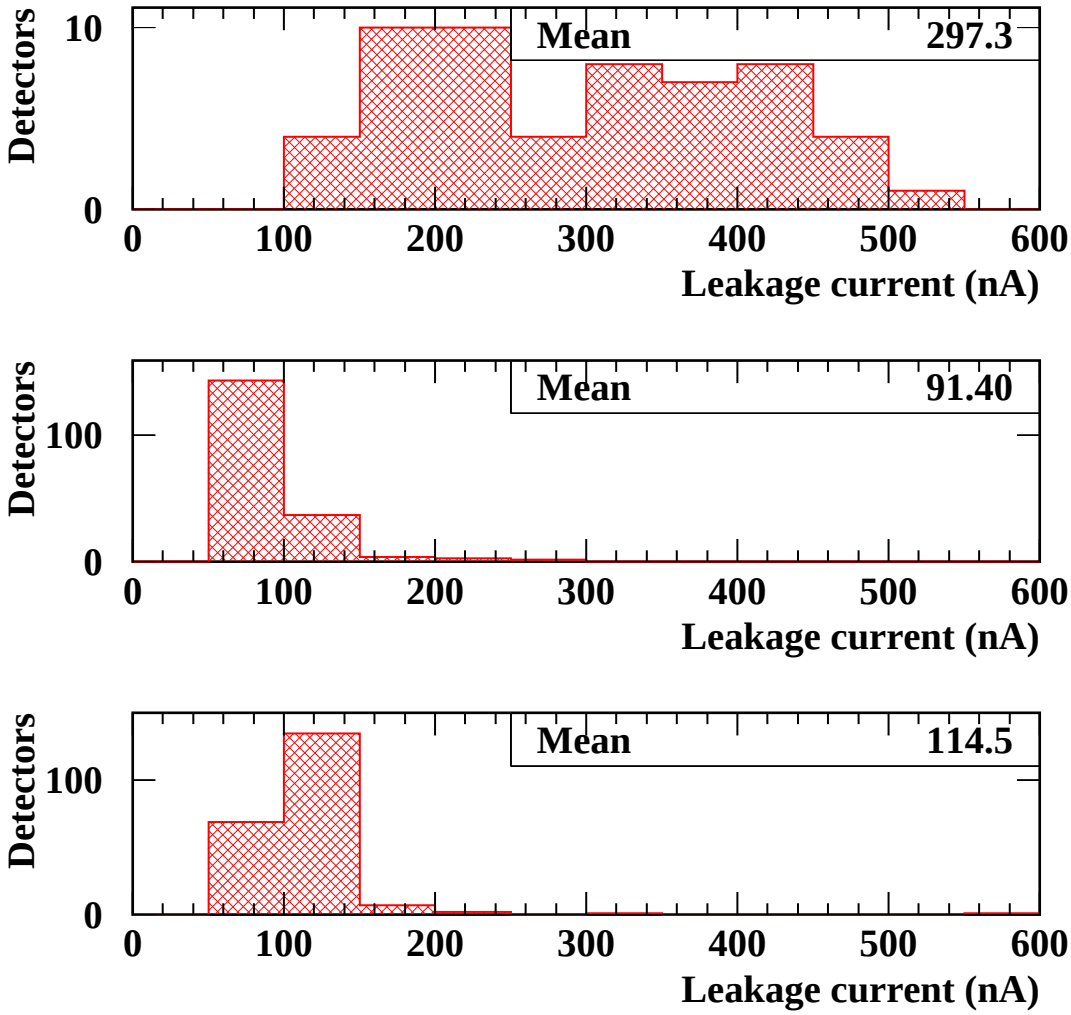


Figure 4: Leakage current for all detectors measured by the GLAST Collaboration: first batch from 4–inch wafers (top), second batch of 4–inch wafers (middle) and batch of 6–inch wafers (bottom).

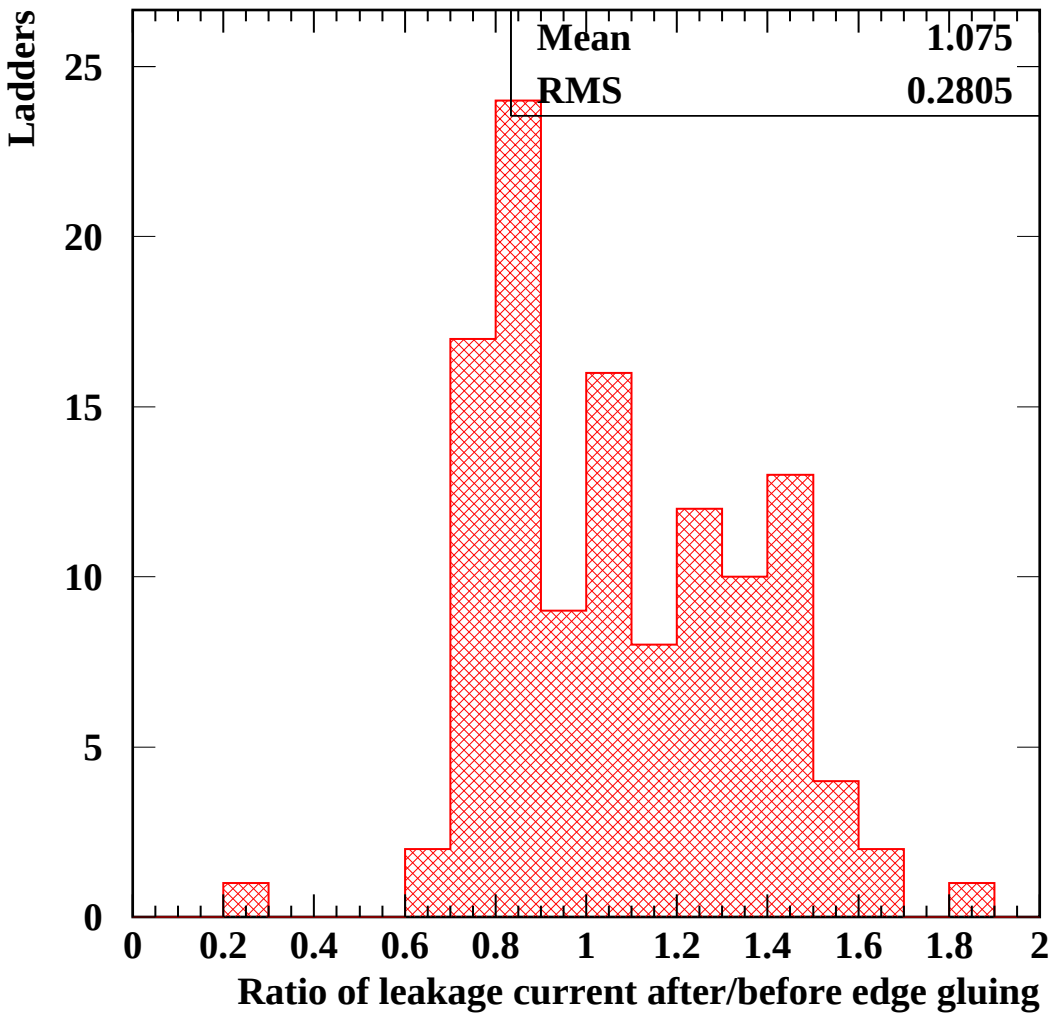


Figure 5: Ratio of ladder currents after and before edge gluing (two ladders are not shown)

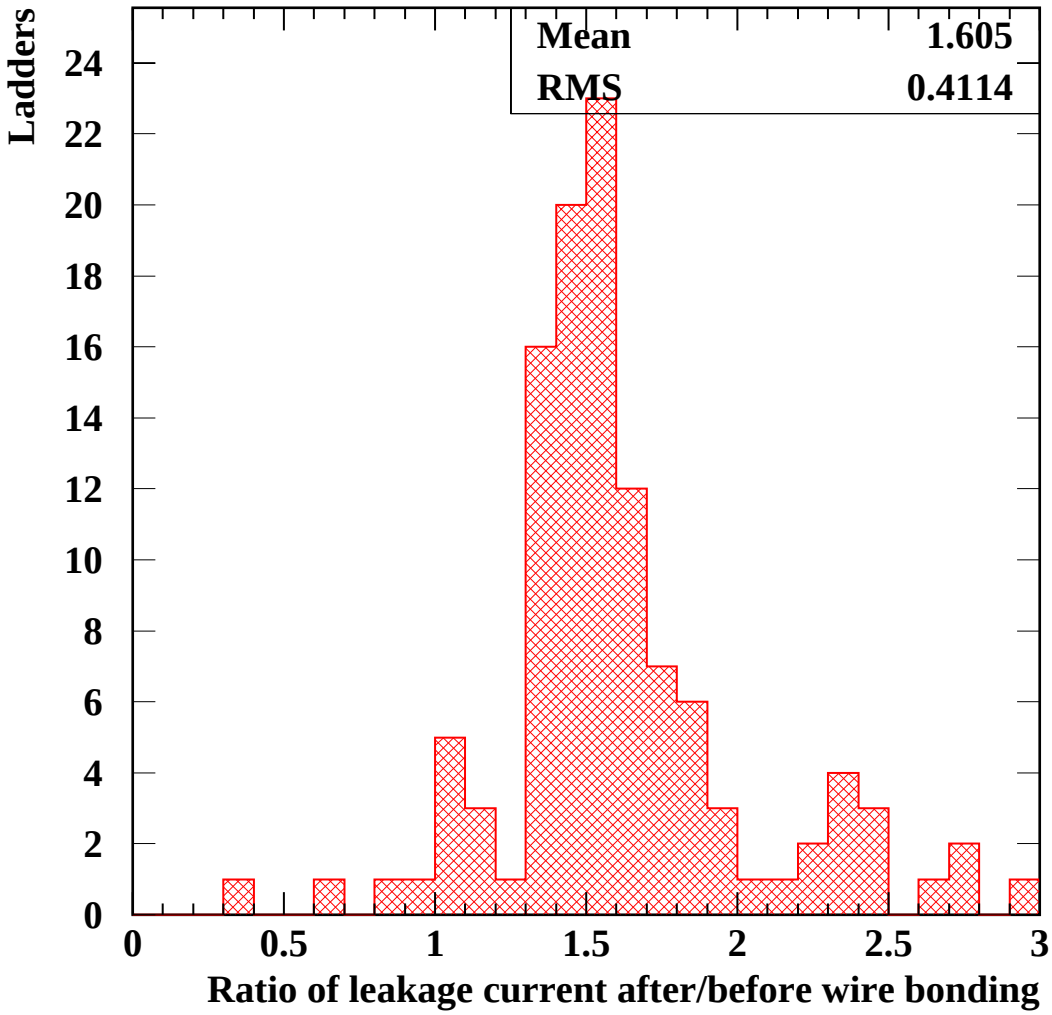


Figure 6: Ratio of ladder currents after and before wire bonding (fifteen ladders are not shown).

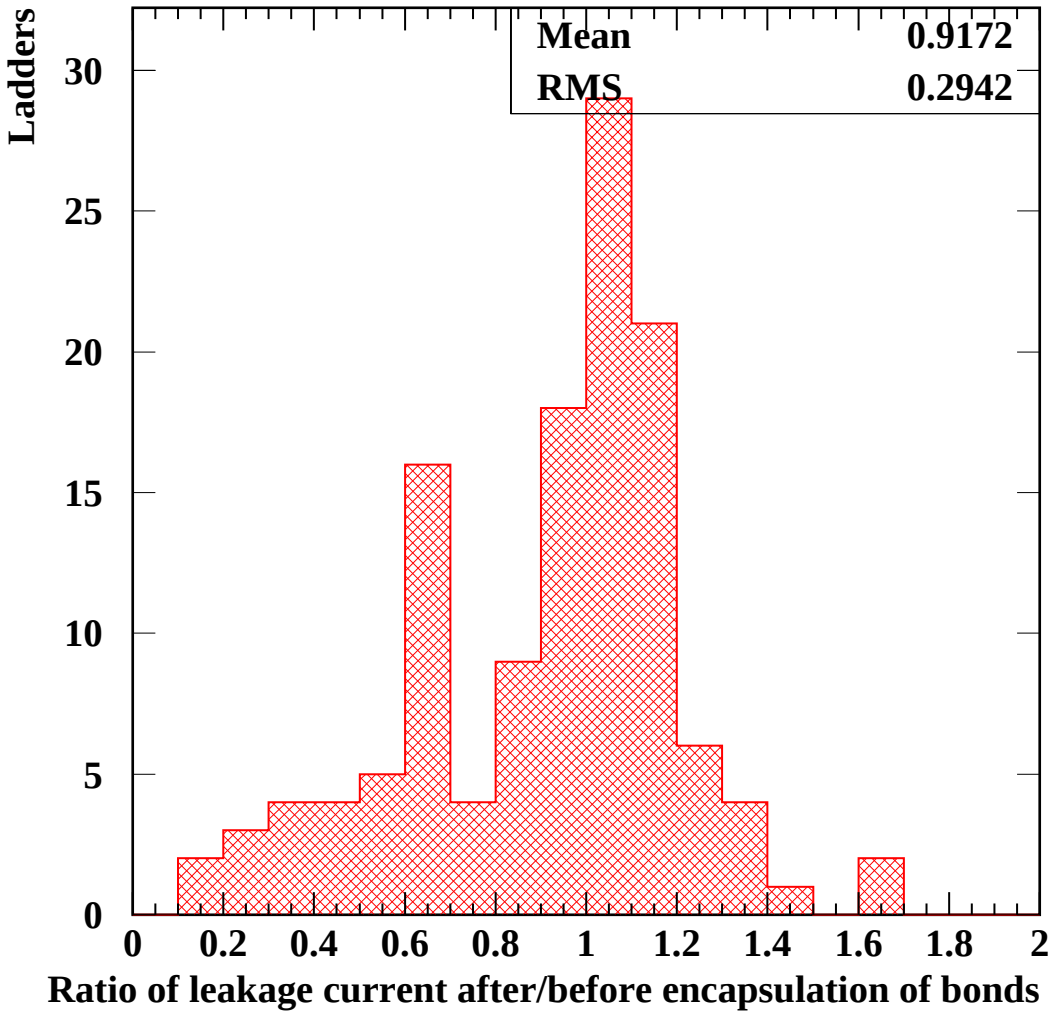


Figure 7: Ratio of ladder currents after and before encapsulation of wire bonds (five ladders are not shown).

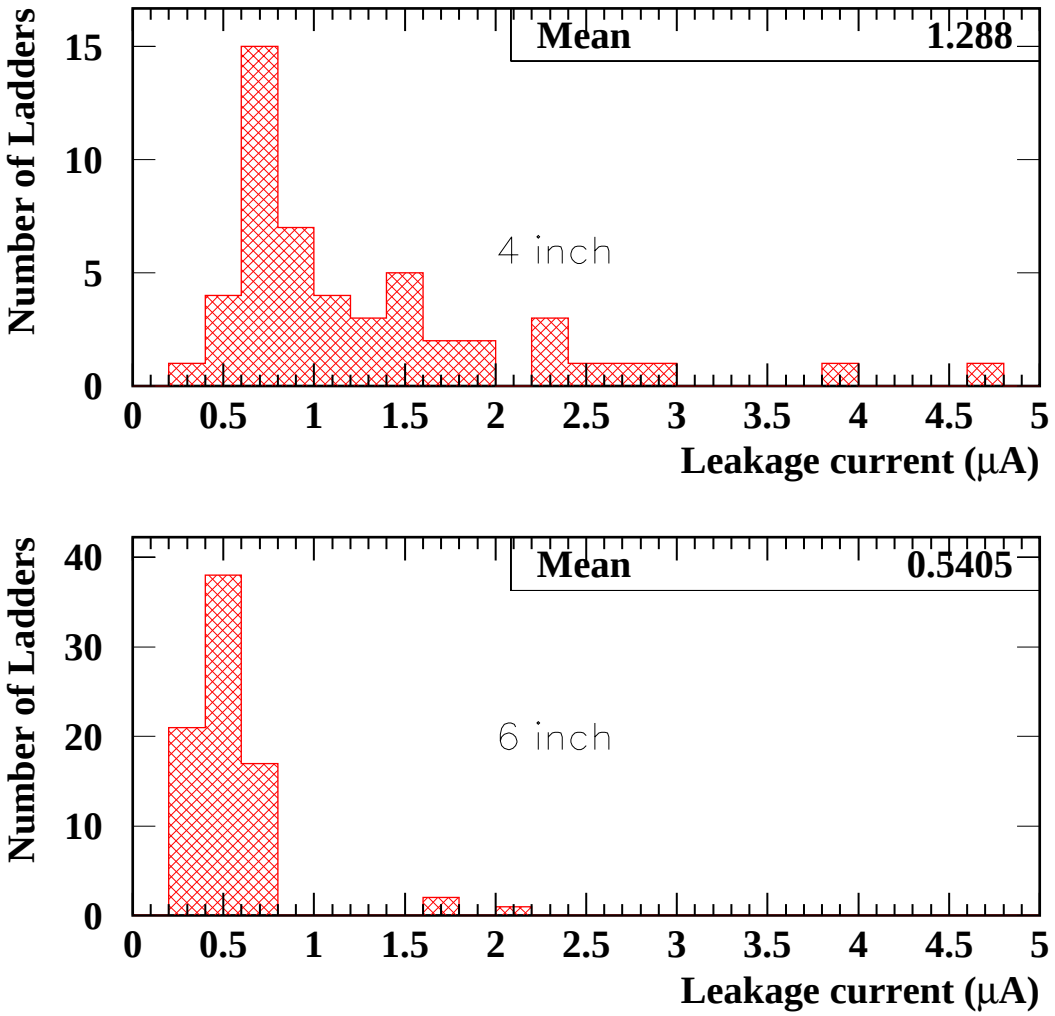


Figure 8: Leakage current for 4–inch (top) and 6–inch (bottom) ladders with leakage current less than 5 $\mu$A after ladder assembly. Ladders with higher currents are listed in Table 1.

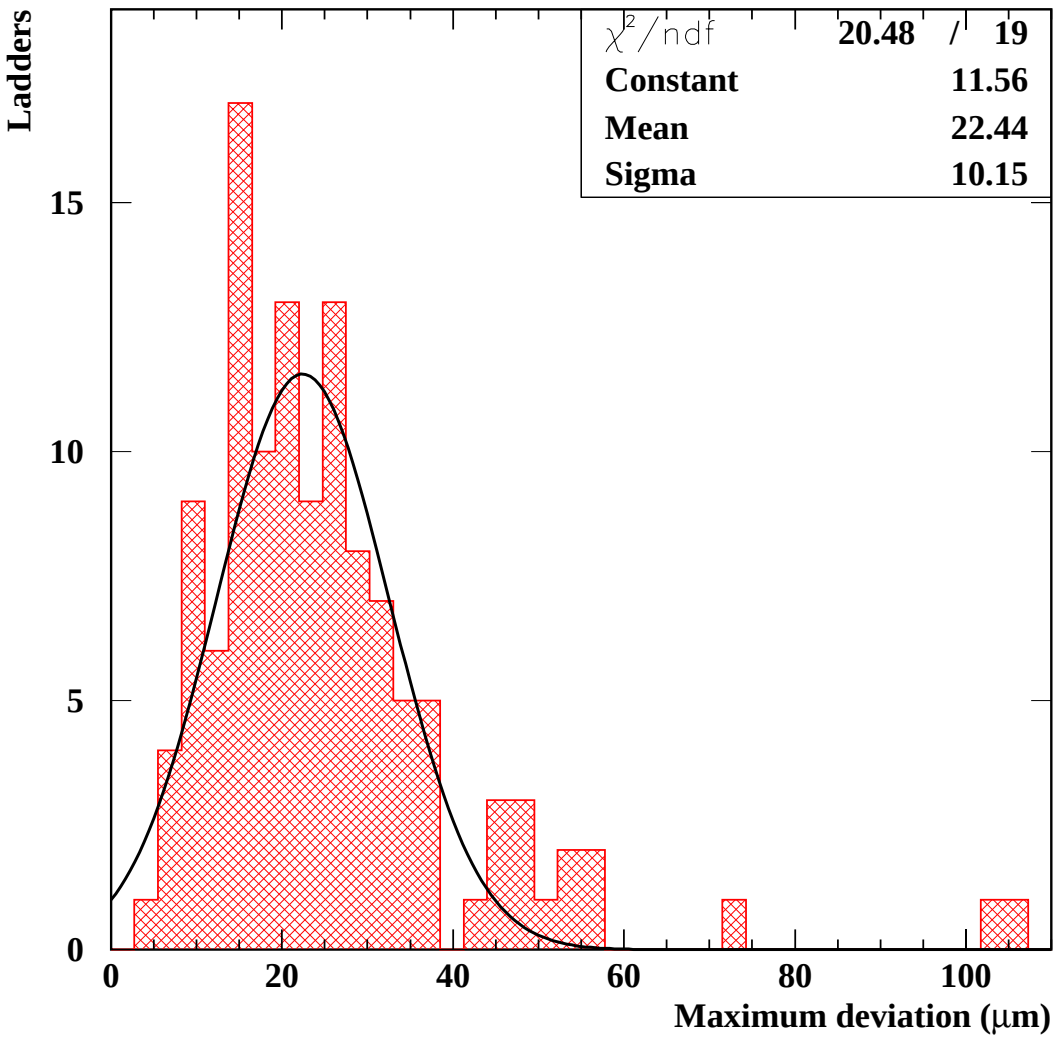


Figure 9: Alignment of detectors in a ladder.

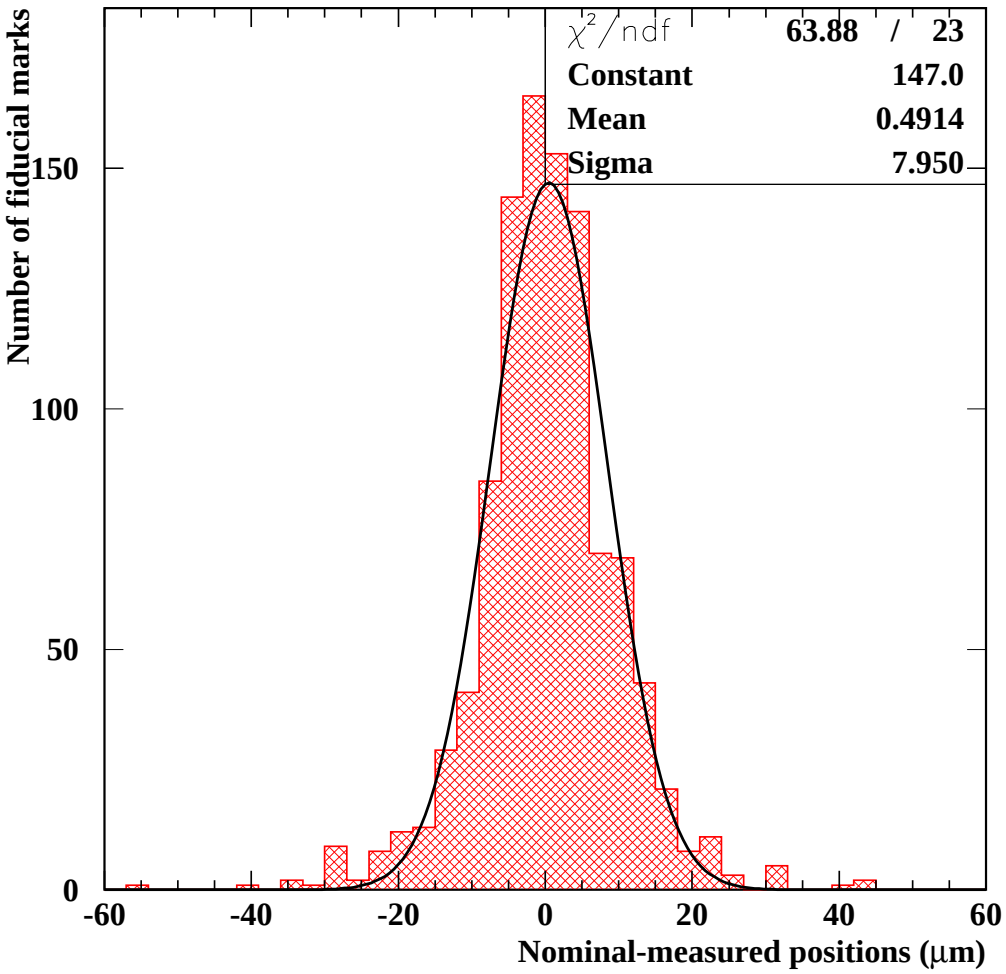


Figure 10: Difference between nominal and measured position for all detector fiducial marks along the direction perpendicular to the strips.